Subpicosecond Ring Opening of 7-Dehydrocholesterol Studied by Ultrafast Spectroscopy

Neil A. Anderson, Joseph J. Shiang, and Roseanne J. Sension*

Department of Chemistry, University of Michigan, Ann Arbor, Michigan 48109-1055

Received: July 1, 1999; In Final Form: October 4, 1999

The photoinitiated electrocyclic ring opening of 7-dehydrocholesterol (DHC) to form previtamin D_3 was studied in methanol solution with femtosecond transient absorption spectroscopy. The molecules were excited at 265 nm and probed at 20 wavelengths ranging from 261 to 650 nm. A sizable absorption signal decaying on a 0.95 ± 0.10 ps time scale was seen at all probe wavelengths from 470 to 650 nm. This absorption is assigned to an $S_1 \rightarrow S_n$ transition that peaks near 470 nm. Thus, the S_1 state has a lifetime of 0.95 ps, while the initially prepared S_2 state has a lifetime ≤ 0.1 ps. Data obtained with probe wavelengths in the ultraviolet yielded a subpicosecond (0.4−1.0 ps) component corresponding to the lifetime of the S_1 state. This data set also exhibits a 1−5 ps wavelength-dependent component assigned to vibrational cooling, and a 100 ± 20 ps component assigned to rotational isomerization of the photoproduct to achieve a thermal distribution of rotamers. No further dynamics are seen for time delays of up to 1 ns. Agreement between the static difference spectrum and the absorption difference observed in the kinetic data at 300 ps indicates that there are no significant longer-time dynamics.

Introduction

The photochemical formation of vitamin D has been a subject of much interest from a biological as well as a synthetic standpoint.[1−2] Photochemical synthesis of vitamin D is complicated by overlapping absorption bands for products and reactants that cause both reversible and irreversible formation of undesirable products. A great deal of effort has been expended to investigate mechanisms for improving product yield.[3−5] However, the mechanisms at all points of the synthesis are not completely understood. The photochemical reactions occur quickly, making them difficult to study. Direct observation of the various reactions can provide information about the mechanisms involved and may ultimately yield information about how to control the reactions to achieve the desired products. As a step in understanding the mechanisms in this system, we present here a time-resolved study of the initial step in vitamin D_3 formation.

The initial step in the formation of vitamin D_3 is the electrocyclic ring opening of 7-dehydrocholesterol (DHC) to form previtamin D_3. This reaction is initiated by absorption of a photon of ultraviolet light and occurs with a quantum yield of 34% (Scheme 1).[6] The previtamin product can exist in two important conformers. Immediately following ring opening, the previtamin will be formed in the all-s-cis (cZc) conformation. Subsequent rotation around one of the single bonds in the chromophore results in the formation of a mono-s-trans configuration (cZt). Steric hindrance prevents isomerization around the other single bond.

Previtamin D is itself unstable to ultraviolet light and can undergo several photochemical reactions (Scheme 2). Ring closure can occur, forming DHC or lumisterol. Double bond cis−trans isomerization can also occur to form tachysterol. The distribution of these photoproducts changes with irradiation wavelength. Ring closure products are favored at longer wavelengths on the edge of the previtamin D absorption band.[6−8] The cZc rotamer is believed to be the precursor to the ring closure products.[2,9] The wavelength dependence can be explained by preferential excitation of cZc previtamin D at longer wavelengths and by the presence of competitive pathways leading to ring opening and isomerization on the cZc excited state surfaces.[10]

SCHEME 1: Formation of Vitamin D[a]

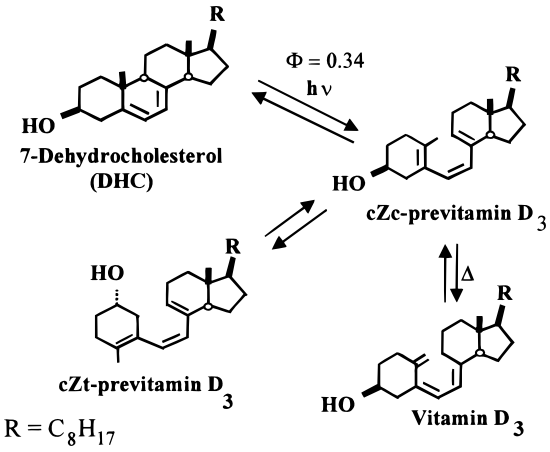

[a] 7-Dehydrocholesterol undergoes an electrocyclic ring opening to form previtamin D, which can exist in an all-s-cis (cZc) or a mono-s-trans (cZt) rotamer. Vitamin D is formed from the cZc rotamer of the previtamin via a thermally activated hydrogen shift.

The final step to form vitamin D from the previtamin is a thermally activated hydrogen shift in the cZc rotamer, rather than a photochemical process. Therefore, for optimal vitamin D synthesis, the desired photochemical process will result in a maximization of the previtamin D species available for thermal conversion to produce the final product.

The DHC ring-opening reaction is completely analogous to the extensively studied ring opening of 1,3-cyclohexadiene to form 1,3,5-*cis*-hexatriene.[11−20] In this reaction, the initially excited S_2 (1^1B_2) state of cyclohexadiene decays in about 43 fs to a doubly excited S_1 (2^1A_1) state with the same symmetry as the ground state.[20] The S_1 state decays nonradiatively on a

10.1021/jp992267u CCC: $18.00
Published on Web 11/12/1999

SCHEME 2: Reversible Photochemistry of Previtamin D[a]

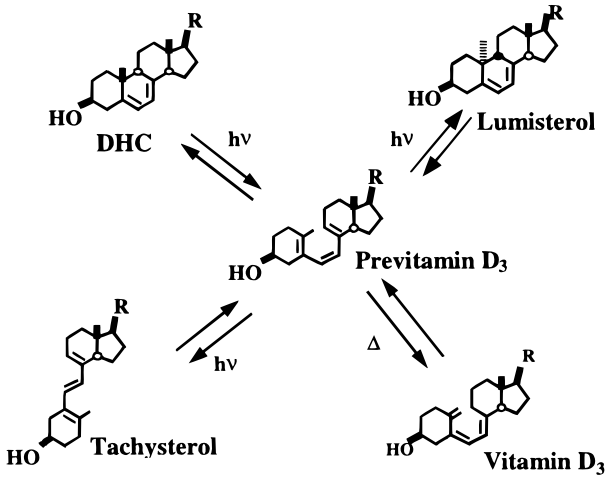

[a] The previtamin can undergo ring closure to form 7-dehydrocholesterol or lumisterol. Alternatively, cis−trans isomerization around the central double bond of the hexatriene reaction center results in tachysterol formation.

subpicosecond time scale to the ground state manifold. This efficient ultrafast decay is made possible by the presence of conical intersections connecting the potential surfaces. These intersections have been characterized theoretically and found to be accessible with no significant barrier on the excited state surface.[21] Branching to form photoproduct is believed to occur immediately after passing through the conical intersection, so that the excited state lifetime and the rate of reaction are effectively identical. Therefore, the cyclohexadiene ring-opening reaction occurs on a time scale of <500 fs in solution.[17−20]

Similar conical intersections should be present on the DHC excited state surfaces. However, their accessibility will depend on the influence of the added substituents on the critical modes and the presence or absence of barriers between the Franck−Condon excited region and the conical intersection. In fact, the presence of conical intersections has been theoretically documented for ergosterol, the precursor to vitamin D_2, which differs only slightly from DHC in structure.[22]

Thus far, very few time-resolved photochemical studies have been conducted on DHC. In a recent study, the ring-opening reaction was assigned to a 5.2 ps component observed in deep UV transient absorption data.[23] This time constant was in good agreement with the 6 ps time constant that was generally accepted for the 1,3-cyclohexadiene ring-opening reaction at that time.[13] In view of more recent data demonstrating a subpicosecond return to the ground state for the model system,[17−20] we have undertaken a re-examination of the photochemistry of DHC. In this paper, we present a study of the photochemical ring opening of DHC, employing ultrafast transient absorption techniques covering an extensive range of wavelengths to observe the reaction and the subsequent cooling and relaxation dynamics from 200 fs to 1 ns.

Experiment

The photoinitiated reaction of 7-dehydrocholesterol to form previtamin D_3 was studied using pump−probe transient absorption spectroscopy. The molecules were excited at 265 nm and probed at 20 wavelengths from 261 to 650 nm. Except for anisotropy measurements, all scans were carried out with the relative polarizations of the pump and probe beams at the magic angle of 54.7° to eliminate contributions due to changes in the orientation of the probed transition dipole.

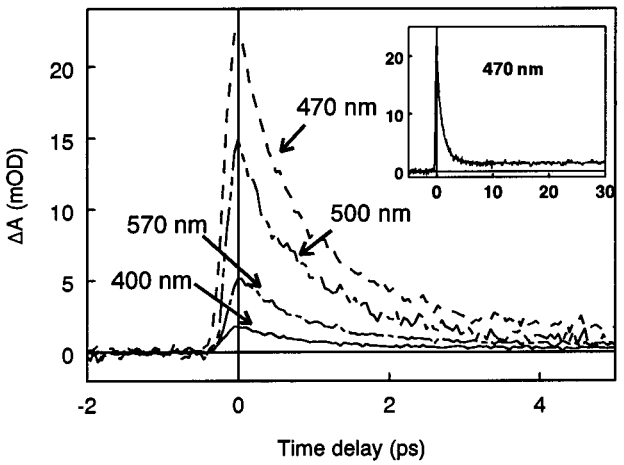

Figure 1. Time-resolved absorption dynamics observed at 400, 470, 500, and 570 nm following excitation of DHC at 265 nm. The inset shows kinetic data probed at 470 nm over a longer, 30 ps, time range. The visible probe data from 470 to 650 nm fit to a single-exponential component (0.95 ± 0.10 ps) convoluted with an instrument limited solvent spike and slight persistent absorption.

The output of a home-built 1 kHz regeneratively amplified titanium sapphire laser was split to provide pump and probe beams. For all scans, the third harmonic of the laser at 265 nm was generated as the pump beam. Pump energy at the sample was 300−600 nJ/pulse. Experiments were typically carried out with a 150 fs fwhm pulse at the sample. A tunable ultraviolet probe was generated by frequency doubling the output of a home-built optical parametric amplifier[24] in a BBO crystal. In all, 13 UV probe wavelengths ranging from 261 to 340 nm were used. The OPA output was taken directly to produce the six probe wavelengths from 470 to 650 nm. The second harmonic of the laser was taken to produce the 400 nm probe. In all cases, the probe beam was attenuated to be <10% of the pump beam intensity. This experimental setup has been described in detail previously.[25] The data were collected using digital noise reduction procedures.[26]

7-Dehydrocholesterol (Aldrich) was used as received and dissolved in methanol (Mallinckrodt 99.9% HPLC grade) at a concentration of $\sim 1 \times 10^{-3}$ M. Experiments were carried out at 295 K. The sample was flowed through a 1 mm path length cell to refresh the volume between laser shots. Static absorption spectra of samples were taken before and after use to ensure that the samples had not degraded substantially through a buildup of the previtamin photoproduct.

Results

A. Visible Probe Kinetics (470−650 nm). Six kinetic traces taken with probe wavelengths from 470 to 650 nm all exhibit very similar behavior (see Figure 1). An instrument-limited rise is followed by a decay to a residual absorption that is constant over the 10 ps window studied. The residual is typically <10% of the intensity of the initial absorption. An instrument-limited Gaussian spike is observed in addition to the picosecond component for probe wavelengths less than 540 nm.

Solvent-only scans were taken to separate solvent from solute signals. A comparison of solvent only and solvent plus solute scans is shown in Figure 2. An instrument-limited Gaussian spike is observed in solvent-only scans of methanol when probing at all wavelengths less than 540 nm. In addition, all solvent-only scans show a slight persistent absorption with an

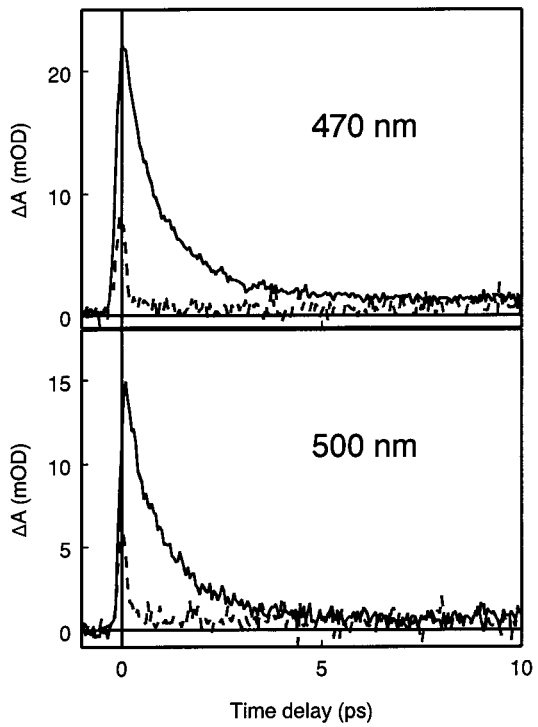

Figure 2. Transient absorption kinetic scans of DHC in methanol probed at 470 and 500 nm are shown with solid lines. The dashed line in each frame is signal observed in solvent-only scans at the indicated wavelengths. The spikes in the solvent-only scans are pulse width limited, indicating that the rise of the DHC absorption is also very nearly pulse width limited. The absorption pedestal seen in the solvent-only scans is similar in amplitude to that seen in solvent plus solute scans.

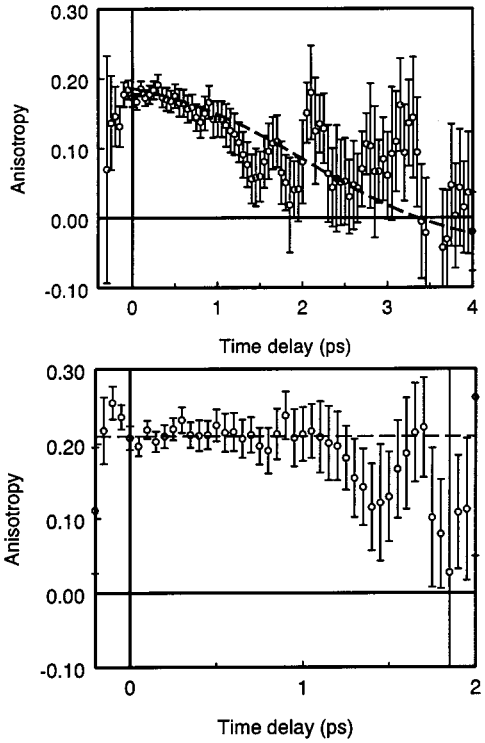

Figure 3. Anisotropy calculated from parallel and perpendicular scans at 600 nm probe wavelength. The upper frame shows the raw anisotropy. The initial value is 0.18 ± 0.01, and it decays to a -0.03 ± 0.05 anisotropy at longer times. The lower frame shows the anisotropy recalculated after subtracting the persistent absorption component from the signal. In this case, the initial anisotropy is 0.21 ± 0.01 and no decay is observed.

apparently instrument-limited appearance, and no decay on a 10 ps time scale. This persistent absorption is similar in amplitude to the absorption pedestal seen in the DHC/methanol scans. No other dynamics are observed in the solvent-only scans. Therefore, the picosecond decay process seen in Figures 1 and 2 can be definitively assigned to the solute.

The pump power response of the picosecond component was tested at 570 nm. This wavelength was chosen to avoid contributions from the instrument-limited spike. Reducing the pump intensity by 55% resulted in a $59 \pm 5\%$ decrease in the initial signal, supporting the hypothesis that the picosecond process arises from the absorption of a single pump photon by DHC.

The absorption responsible for the decaying component appears to peak strongly near 470 nm. The signal probed at 650 nm is weak (1.7 mOD), and the signals grow progressively larger at shorter probe wavelengths. The initial signal at 470 nm probe (excluding the solvent spike) is ~15 mOD, which is twice the size of any other signal with visible probe. The amplitude of the 400 nm signal is much less than that of the 470 nm signal.

Scans between 470 and 650 nm were fit using a global analysis routine, to a model consisting of an instrument-limited Gaussian spike (for probe wavelengths less than 540 nm), a single-exponential decay, and a nondecaying component. The exponential decay constant derived from this fit is 0.95 ± 0.10 ps. Altering the model to allow a second exponential decay did not improve the quality of the fit.

In addition to the magic-angle traces, an anisotropy measurement was made at a probe wavelength of 600 nm to obtain further information about the species responsible for the absorption (upper frame of Figure 3). This wavelength was chosen because it was free of the solvent spike, seen at shorter probe wavelengths, which could obscure the initial anisotropy of the solute. The initial anisotropy of 0.18 ± 0.01 decays on a 0.9 ± 0.2 ps time scale. The anisotropy of the long-lived absorption is -0.03 ± 0.05. Using our global analysis results to partition the data into fast (0.95 ps) and slow components, we determine the anisotropy in the absence of the persistent absorption. This is shown in the lower frame of Figure 3. In this case, the initial anisotropy is 0.21 ± 0.01 and no significant decay is seen within the first 1.8 ps. After that time, the anisotropy becomes very noisy and can no longer be resolved, in conjunction with the disappearance of the signal.

B. Ultraviolet Probe Wavelengths (261−400 nm). Kinetic traces were taken at 14 probe wavelengths from 261 to 400 nm. This covers a substantial portion of the DHC absorption band (Figure 4) and also extends 100 nm to the red of the absorption region. Sample transient absorption kinetics are shown in Figure 5. Most scans extend to a time delay of 300 ps, although scans at 277 and 312 nm extend to 1 ns. A pulse width limited spike in absorption at zero time delay is again observed in all scans and also appeared in scans of methanol alone.

The signal observed immediately after the spike is a photobleach at 261−295 nm, and an absorption from 300 to 400 nm. The ensuing dynamics occur on multiple time scales. The longest component observed is 100 ± 20 ps. This component is typically small in amplitude and is not clearly resolved at all wavelengths. The 100 ps component corresponds to an increase in absorption when observed at all probe wavelengths less than 297 nm. It corresponds to a decrease in absorption at wave-

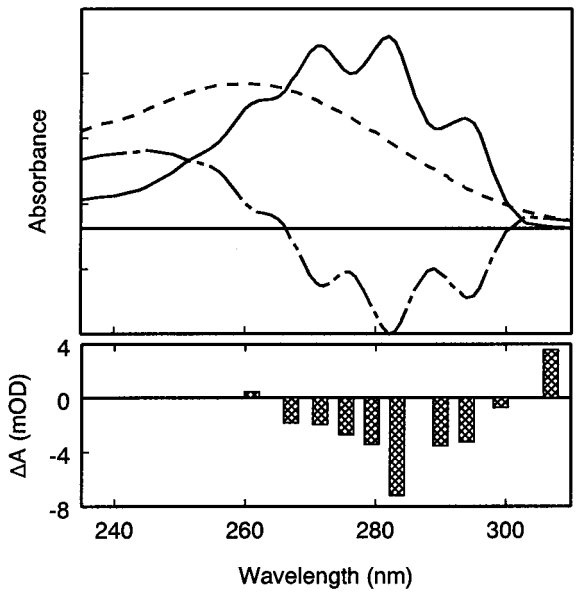

Figure 4. The static absorption spectrum of DHC is shown as the solid line in the upper frame. The dashed line is the static spectrum of previtamin D. The dot−dash line corresponds to the difference between the two static spectra. The lower frame shows the absorption difference actually observed at 300 ps. Because the kinetic traces were obtained on different days, under slightly different conditions, the relative intensities are qualitatively, but not quantitatively precise. The qualitative agreement with the shape of the static difference spectrum, as well as the quantitative agreement of the zero crossing points, indicates that all major dynamics are complete within 300 ps.

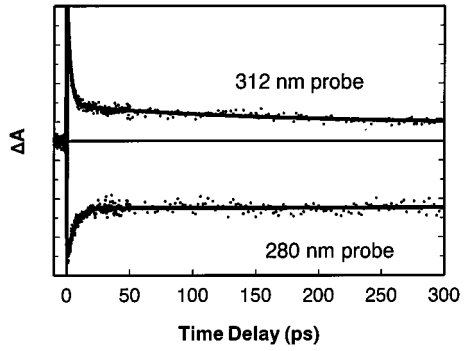

Figure 5. Time-resolved absorption dynamics observed at 280 and 312 nm following excitation of DHC at 265 nm. The 312 data exhibit a biexponential decay of 2.7 and 110 ps. The solid lines represent fits to the data. The 280 nm kinetic is modeled by a subpicosecond component and a 5.6 ps component. Both fits also contain a Gaussian spike that represents the instrument-limited spike seen in solvent-only scans.

lengths greater than 297 nm. No longer dynamics are seen in the scans extending to 1 ns.

The magnitudes of the transient absorption signals observed at 300 ps are shown in the lower frame of Figure 4. The shape of these data is in qualitative agreement with the static difference spectrum shown in the upper frame. The wavelengths at which the difference spectra cross zero are in quantitative agreement. The observed signal at 300 ps crosses from an absorption increase to a bleach between 261 and 267 nm and crosses back to a net absorption increase between 299 and 307 nm. The crossing points of the static DHC and previtamin spectra occur at 266 and 301 nm.[27] The agreement of the 300 ps and static difference spectra and the lack of longer dynamics in scans to 1 ns indicate that there are no significant dynamic processes occurring on time scales longer than 100 ps.

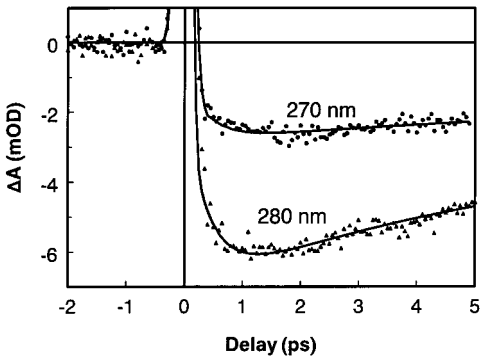

Figure 6. Early time dynamics observed at 270 and 280 nm. Following the solvent spike, the subpicosecond component is seen as a slight growth of the bleach. The bleach then decays on a 5 ± 0.7 ps time scale.

When probing in the absorption band from 261 to 285 nm, two faster components are resolved at earlier time delays. A subpicosecond growth of the bleach is followed by a 5.0 ± 0.7 ps decay. The early time behavior probing in the absorption band is shown in Figure 6. The time scale of the subpicosecond component is difficult to fit exactly because the amplitude of the solvent spike is so large at these wavelengths. The solvent spike is modeled as a Gaussian, but even a slight deviation from ideal behavior will affect the apparent time scale of this small component. As a result, the component can be fit with time constants ranging from 0.4 to 1.0 ps.

At UV wavelengths longer than 285 nm, the subpicosecond component is no longer clearly resolved. The remaining kinetics in the absorption band can be fit with a single 5.0 ± 0.7 ps component and the 100 ps component discussed earlier. Scans from 307 to 400 nm, outside the DHC absorption band, can also be fit with one fast component. However, the time scale of this component changes with wavelength. It fits to 3.3 ps at 307 nm and drops steadily to 1.3 ps at 340 and 400 nm.

Discussion

The data presented above show dynamics on three distinct time scales. A subpicosecond component is observed when probing between 261 and 285 nm and also when probing in the visible. A large amplitude 1−6 ps component is observed at all UV probe wavelengths. Finally, a 100 ps component with small amplitude is also seen in most of the UV data. We now present a model to describe the observed data. The components will be considered in order from longest to shortest.

A. Conformational Relaxation of the Photoproduct (100 ps). As noted previously, previtamin D_3 can exist in two basic rotamers, cZc and cZt. The energies of these rotamers have been calculated to lie within a few hundred wavenumbers of each other with cZc previtamin D thought to be slightly more stable.[28] Therefore, the thermally equilibrated previtamin D population is expected to contain a substantial population of both cZc and cZt previtamin D. However, the ring opening of 7-dehydrocholesterol will not form an equilibrium distribution of rotamers immediately. The cZc rotamer will be formed first, then a thermal distribution will be established through rotational isomerization from the cZc rotamer to the cZt rotamer.

A previous time-resolved study by Fuss et al. in ethanol solvent reported a 60−1300 ps temperature-dependent decay. This decay was assigned to rotational isomerization from cZc to cZt previtamin D. An Arrhenius analysis of that data gave a barrier of 15.5 ± 1 kJ/mol.[23] This barrier agrees well with single bond rotational isomerization barriers in short chain polyenes.[29,30]

The 100 ± 20 ps component found in the current study is consistent with the rate constant predicted by Fuss et al. in ethanol solution for a temperature of 295 K.[23] The large range of probe wavelengths presented here allows us to comment further on the spectral behavior of this component.

Assigning the 100 ps decay component to rotational isomerization of the previtamin means that a nearly thermal distribution of previtamin rotamers should be present at 300 ps. If so, the observed difference spectrum at 300 ps should be very close to the difference between the static DHC and previtamin D spectra. The bottom frame of Figure 4 shows that the 300 ps data approximates the static difference spectrum well. As a result of this agreement, we therefore expect to observe no significant longer dynamics in the system and indeed saw none when scanning out to 1 ns time delay at 277 or 312 nm.

The 100 ps decay component observed in the data corresponds to an absorption increase at wavelengths less than 297 nm and an absorption decrease at wavelengths greater than 297 nm. Therefore, it reflects a blue shift of the observed composite spectrum. Assigning this component to rotational isomerization requires that cZt previtamin D has an absorption spectrum that is blue-shifted with respect to the spectrum of the initially formed cZc rotamer.

Studies of the wavelength-dependent photochemistry of previtamin D provide evidence for such a blue-shifted cZt spectrum. Previtamin D can undergo a photoinduced cis−trans isomerization to form tachysterol. It also undergoes photoinduced ring-closure reactions to form dehydrocholesterol and lumisterol. However, the ring-closure products are postulated to form only from the cZc rotamer.[2,9] A number of experiments have shown that the quantum yield for ring closure increases and isomerization decreases at longer irradiation wavelengths.[6−8] This increase in ring closure was originally postulated to result from preferential excitation of the cZc rotamer at longer wavelengths.[7] However, a careful study of a range of irradiation wavelengths showed that a more complex description of the wavelength dependence was necessary.[8] A recent study by Fuss and Lochbrunner presents a spectrum for cZc previtamin D at low temperature that is red-shifted a few nanometers from the cZt spectrum. The wavelength dependence of the observed photochemistry is explained by preferential excitation of cZc at wavelengths longer than 300 nm and by the presence of two competitive cZc previtamin D excited state pathways. One of the excited state pathways leads to ring closure, while the other leads to cis−trans isomerization. The presence of a slight barrier on the isomerization pathway and no barrier for ring closure explains the effects of irradiation wavelength on the photochemistry of previtamin D.[10]

In summary, the present work provides further corroboration for the assignment of the temperature-dependent decay reported by Fuss et al. to rotational isomerization.[23] The spectral blue-shift deduced from this component is consistent with the rotamer spectra. The data indicates that the cZt previtamin D rotamer is a stronger absorber at wavelengths from 261 to 297 nm, while the cZc rotamer absorbs more strongly beyond 297 nm. In addition, the difference spectrum at 300 ps approximates the static difference spectrum for the formation of an equilibrium distribution of rotamers.

B. Vibrational Cooling (1−5 ps). Transient absorption scans in the UV absorption band exhibit a 5.0 ± 0.7 ps component and a subpicosecond component in addition to the 100 ± 20 ps component discussed in the previous section. The 5 ps component is consistent with the 5.2 ± 0.5 ps component assigned by Fuss et al. to the time scale for ring opening.[23] However, in the present data set, we find that the time scale of this component varies with wavelength outside the absorption band, becoming faster at redder wavelengths. The observed rate corresponding to a reaction or state transition will not generally vary with wavelength. Furthermore, an additional subpicosecond component is observed in the visible and UV data. These observations suggest that the "5 ps" component does not correspond to return to the ground state.

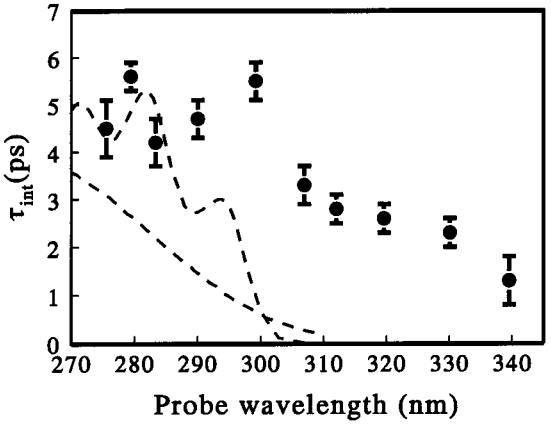

Figure 7. Values for the time constant of the 1−5 ps component as a function of wavelength. The static absorption spectra of DHC and previtamin D (broken lines) are overlaid for wavelength reference. The 1−5 ps component remains relatively constant through the absorption band of DHC and previtamin D. At longer wavelengths outside the absorption band, the component becomes faster.

Figure 7 shows the wavelength evolution of the time scale of this component. Within error, the time scale remains constant throughout the absorption band of DHC. However, it clearly becomes faster at longer wavelengths outside this region. A gradual trend is seen from 3.3 ps at 307 nm down to 1.3 ps at 340 and 400 nm. The wavelength dependence suggests that this component arises from vibrational cooling. Cooling components are expected to show wavelength dependence, as they result from a gradual spectral evolution rather than a transformation between two distinct spectra. Furthermore, a cooling component will generally increase in rate when probed at wavelengths farther from the absorption maximum. The cooling seen here must be occurring on the ground state because there is no longer decay component that could be assigned to return to the ground state. Finally, the 1−5 ps component corresponds to an absorption decrease from 290 to 400 nm and an increase at shorter wavelengths. These observations are consistent with evolution from the broadened spectrum expected at early times for a vibrationally excited species to a narrower spectrum after cooling.

DHC absorbs light energy into the cyclohexadiene chromophore. Therefore, energy will initially be localized in the chromophore. This energy will then be redistributed throughout all of the modes of the molecule via intramolecular vibrational energy redistribution (IVR) and eventually lost to the solvent. Both of these processes may contribute to the observed signal. The DHC and previtamin D molecules will both undergo this redistribution of energy after return to the ground state, possibly on slightly different time scales. Because DHC has a stronger, more structured absorption than previtamin D and accounts for the majority (ca. 66%) of the population after reaction, the observed cooling signal will be dominated by DHC.

C. Ultrafast Ring Opening and Return to the Ground State (0.95 ps). Following excitation of DHC, a subpicosecond process is observed with probe wavelengths both in the UV absorption band and in the visible. The visible absorption signal

is quite strong, with an intensity peak near 470 nm. These data fit quite well to a single-exponential decay of 0.95 ± 0.10 ps and a small persistent absorption pedestal. There are three possible assignments for the 0.95 ps component. This component may be assigned to the relaxation of vibrationally hot previtamin D_3 produced after ring-opening, the relaxation of vibrationally hot DHC produced following internal conversion to the ground state, or an excited state absorption decaying by internal conversion.

Vibrational cooling of either DHC or previtamin D_3 should be characterized by a signal that decreases monotonically to the red of the static absorption band. In addition, the rate of relaxation will generally increase as the wavelength moves away from the static absorption band. These properties are observed for the signal identified above as vibrational cooling. However, the rate of decay of the visible absorption band is nearly constant between 470 and 650 nm. In addition, the observed signal exhibits a strong increase in intensity between 400 and 470 nm. These facts make assignment to absorption from vibrationally hot molecules improbable. Therefore, this signal must arise from an excited state absorption. It should be noted that a similar visible absorption has been reported for cyclohexadiene and both hexatriene isomers in solution and assigned to the $S_1 \rightarrow S_n$ transition.[18,31]

The excited state absorption probed at wavelengths between 400 and 650 nm could originate from the initially prepared S_2 state or from the S_1 state following internal conversion. After excitation of 1,3-cyclohexadiene, the lifetime of the initially prepared S_2 (1^1B_2) state is only 43 fs.[10] The short lifetime of the S_2 state in the model cyclohexadiene compound, along with the absence of a longer component in the present data set that could correspond to the S_1 lifetime leads us to postulate that the 0.95 ps decay corresponds to decay from the S_1 state to the ground state. The rise of the visible absorption attributed to $S_1 \rightarrow S_n$ appears to be pulse width limited. The absence of an observable rise on the excited state absorption leads to the conclusion that either the S_2 lifetime is $<$100 fs or the excited state spectra of the S_1 and S_2 states are similar, obscuring observation of the S_2 to S_1 internal conversion. The latter possibility may be dismissed by consideration of the anisotropy data. It is unlikely that the $S_1 \rightarrow S_n$ and $S_2 \rightarrow S_n$ spectra would have the same polarization and intensity in the visible.

The anisotropy data is presented in Figure 3 for a probe wavelength of 600 nm. The anisotropy, $r(t)$, for a given transition is determined by the average angle between the pumped and probed transition dipoles $\theta(t)$ by

$$r(t) = \frac{2}{5}\langle P_2[\cos\theta(t)]\rangle \qquad (1)$$

where P_2 in eq 1 is the second Legendre polynomial. When more than one species contributes to the observed signal, the composite anisotropy is given by

$$r(t) = \sum_i A_i(t) r_i(t) \qquad (2)$$

where $r_i(t)$ refers to the anisotropy of each of the individual absorbers as given by eq 1 and $A_i(t)$ refers to the fraction of the signal contributed by the ith component. Equation 2 neglects the effects of orientational relaxation in the system, which will cause the anisotropy to eventually go to zero. This is of greater concern in small molecules, where rotation may be rapid. Orientational relaxation is expected to be relatively slow for DHC and previtamin D. An anisotropy measurement performed at a probe wavelength of 284 nm (data not shown) demonstrates that the rotational randomization occurs on a $>$100 ps time scale. Therefore, rotational relaxation can be neglected in the analysis of the visible anisotropy over the first 5 ps.

SCHEME 3: Proposed Reaction Scheme for the Photochemical Ring Opening of DHC Showing Only the Reaction Center of the Molecule[a]

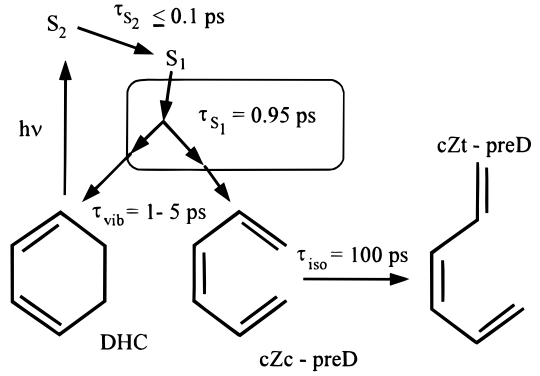

[a] The initially formed excited state is depopulated within 100 fs. The reaction and return to the ground state occur in 0.95 ps. Vibrational cooling then follows on a 1−5 ps time scale. Previtamin D rotational isomerization to achieve a thermal distribution of rotamers occurs in 100 ps.

For the data obtained with a 600 nm probe, there will be at least two species contributing to the anisotropy. Both the decaying absorption and the absorption pedestal will contribute. Therefore, the decay of anisotropy that is observed in the upper frame of Figure 3 is not surprising. This decay is expected as the fraction of the total signal resulting from the subpicosecond component drops. The fact that the decay of the initial anisotropy occurs on a similar time scale to the decay of the initial component suggests that there are only two processes active here. To further investigate the anisotropy of the excited state absorption, the pedestal was subtracted from both the parallel and perpendicular scans at all time delays and the anisotropy was recalculated. The result, displayed in the lower frame of Figure 3, shows that the anisotropy is constant for as long as it can be resolved. This indicates that the 0.95 ps absorption component does not arise from multiple species, leading to the conclusion that the internal conversion from S_2 to S_1 occurs in $<$100 fs. The observed anisotropy is 0.21 ± 0.01 after pedestal subtraction. Equation 1 predicts that this transition corresponds to an average angle of 34° between the pumped and the probed transition dipoles.

The 0.95 ps ground state recovery following excitation of DHC differs from previous studies which assigned time constants of 4.3 ± 0.5 ps[32] and 5.2 ± 0.5 ps.[23] The present study with better time resolution over a broader wavelength range allows for a more accurate assignment of the subpicosecond and picosecond dynamics following photoexcitation of DHC. The rate of reaction is 2−3 times slower than that of 1,3-cyclohexadiene ring opening in solution.[17,20] This is a significant effect, but it does not require major differences in the excited state surfaces along the reaction coordinate. There may be a slightly higher barrier in accessing the DHC conical intersection for return to the ground state, but it is still quite accessible.

Conclusions

The proposed mechanism for the ring opening of 7-dehydrocholesterol is shown in Scheme 3. For the first time, a subpicosecond process has been observed in the initial step of

vitamin D formation via pump−probe ultrafast transient absorption spectroscopy. This 0.95 ± 0.10 ps component is assigned to the lifetime of the S_1 state, which also corresponds to the time scale for the ring-opening reaction. The excited-state absorption $S_1 \rightarrow S_n$ appears to peak around 470 nm and extends beyond 650 nm.

A wavelength-dependent component of 1−5 ps was observed when probing in the ultraviolet. The evolution of the rate, becoming faster at longer probe wavelengths, along with the sign of the signal, corresponding to an absorption increase below 290 nm and an absorption decrease above 300 nm, allows us to assign this component primarily to IVR and thermalization. It is likely that some rotational isomerization of the photoproduct also occurs during this period while the molecule is vibrationally excited.[17−19]

Finally, a small amplitude component of 100 ± 20 ps was observed. Our analysis of this component corroborates a previous assertion that it results from the barrier crossing for rotational isomerization in the product previtamin as the system attains a thermal distribution of rotamers. The wavelength-dependent sign of this component demonstrates that it corresponds to a spectral blue-shift on a 100 ps time scale. This is consistent with the expectation that the initially formed cZc conformer of previtamin D will absorb at longer wavelengths than the cZt conformer.

Acknowledgment. This research was supported in part by a grant from the NSF (CHE-9415772). N.A.A. and J.J.S. were supported by the Center for Ultrafast Optical Science under Grant STC-PHY-8920108.

References and Notes

(1) Dauben, W. G.; McInnis, E. L.; Michno, D. M. In *Rearrangements in Ground and Excited States*; de Mayo, P., Ed.; Academic Press: New York, 1980; Vol. 3, p 81.

(2) Jacobs, H. J. C.; Havinga, E. *Adv. Photochem.* **1979**, *11*, 305.

(3) Braun, M.; Fuss, W.; Kompa, K. L.; Wolfrum, J. *J. Photochem. Photobiol. A* **1991**, *61*, 15.

(4) Malatesta, V.; Willis, C.; Hackett, P. A. *J. Am. Chem. Soc.* **1981**, *103*, 6781.

(5) Dauben, W. G.; Phillips, R. B. *J. Am. Chem. Soc.* **1982**, *104*, 355.

(6) Gliesing, S.; Reichenbächer, M.; Ilge, H.-D.; Fassler, D. *Z. Chem.* **1989**, *29*, 21.

(7) Jacobs, H. J. C.; Gielen, J. W. J.; Havinga, E. *Tetrahedron Lett.* **1981**, *22*, 4013.

(8) Dauben, W. G.; Disanayaka, B.; Funhoff, D. J. H.; Kohler, B. E.; Schilke, D. E.; Zhou, B. *J. Am. Chem. Soc.* **1991**, *113*, 8367.

(9) Pfoertner, K. *Helv. Chim. Acta* **1972**, *55*, 937.

(10) Fuss, W.; Lochbrunner, S. *J. Photochem. Photobiol. A* **1997**, *105*, 159.

(11) Trulson, M. O.; Dollinger, G. D.; Mathies, R. A. *J. Chem. Phys.* **1990**, *94*, 8396.

(12) Trulson, M. O.; Dollinger, G. D.; Mathies, R. A. *J. Am. Chem. Soc.* **1987**, *109*, 587.

(13) Reid, P. J.; Doig, S. J.; Mathies, R. A. *Chem. Phys. Lett.* **1989**, *156*, 163.

(14) Reid, P. J.; Doig, S. J.; Wickham, S. D.; Mathies, R. A. *J. Am. Chem. Soc.* **1993**, *115*, 4754.

(15) Reid, P. J.; Lawless, M. K.; Wickham, S. D.; Mathies, R. A. *J. Phys. Chem.* **1994**, *98*, 5597.

(16) Pullen, S. H.; Walker, L. A., II; Donovan, B. A.; Sension, R. J. *Chem. Phys. Lett.* **1995**, *242*, 415.

(17) Pullen, S. H.; Anderson, N. A.; Walker, L. A., II; Sension, R. J. *J. Chem. Phys.* **1998**, *108*, 556.

(18) Lochbrunner, S.; Fuss, W.; Schmid, W. E.; Kompa, K. L. *J. Phys. Chem. A* **1998**, *102*, 9334.

(19) Anderson, N. A.; Pullen, S. H.; Walker, L. A., II; Shiang, J. J.; Sension, R. J. *J. Phys. Chem. A* **1998**, *102*, 10588.

(20) Trushin, S. A.; Fuss, W.; Schikarski, T.; Schmid, W. E.; Kompa, K. L. *J. Chem. Phys.* **1997**, *106*, 9386.

(21) Garavelli, M.; Bernandi, F.; Olivucci, M.; Vreven, T.; Klein, S.; Celani, P.; Robb, M. A. *Faraday Discuss.* **1998**, *110*, 51.

(22) Bernardi, F.; Olivucci, M.; Ragazos, I. N.; Robb, M. A. *J. Am. Chem. Soc.* **1992**, *114*, 8211.

(23) Fuss, W.; Höfer, T.; Hering, P.; Kompa, K. L.; Lochbrunner, S.; Schikarski, T.; Schmid, W. E. *J. Phys. Chem.* **1996**, *100*, 921.

(24) Wilhelm, T.; Piel, J.; Riedle, E. *Opt. Lett.* **1997**, *22*, 1494.

(25) Pullen, S. H.; Anderson, N. A.; Walker, L. A., II; Sension, R. J. *J. Chem. Phys.* **1997**, *107*, 4985.

(26) Shiang, J. J.; Anderson, N. A.; Sension, R. J. Unpublished result. Anderson, N. A. Ph.D. Dissertation, University of Michigan, Ann Arbor, MI.

(27) Sternberg, J. C.; Stillo, H. S.; Schwendeman, R. H. *Anal. Chem.* **1960**, *32*, 156.

(28) Dmitrenko, O. G.; Terenetskaya, I. P.; Reischl, W. *J. Photochem. Photobiol. A: Chem.* **1997**, *104*, 113.

(29) Carreira, L. A. *J. Chem. Phys.* **1975**, *62*, 3851.

(30) Ackerman, J. R.; Kohler, B. E. *J. Chem. Phys.* **1984**, *80*, 45.

(31) Ohta, K.; Naitoh, Y.; Tominaga, K.; Hirota, N.; Yoshihara, K. *J. Phys. Chem.* **1998**, *102*, 35.

(32) Gottfried, N.; Kaiser, W.; Braun, M.; Fuss, W.; Kompa, K. L. *Chem. Phys. Lett* **1984**, *110*, 335.